

Communication

Emission Enhancement in fs + ns Dual-Pulse LIBS of Cu

Junfeng Shao¹, Yin Zhang^{1,2} and Anmin Chen^{3,*}

- ¹ State Key Laboratory of Laser Interaction with Matter, Changchun Institute of Optics, Fine Mechanics and Physics of Chinese Academy of Sciences, Changchun 130033, China
² University of Chinese Academy of Sciences, Beijing 100049, China
³ Institute of Atomic and Molecular Physics, Jilin University, Changchun 130012, China
* Correspondence: amchen@jlu.edu.cn

Abstract: Femtosecond (fs) and nanosecond (ns) laser pulses have their own advantages and disadvantages in laser-induced breakdown spectroscopy (LIBS). This paper investigated fs + ns (FN) dual-pulse (DP) LIBS, utilizing the respective advantages of two laser pulses in LIBS. Compared to traditional single ns LIBS, applying a smaller energy fs pulse could effectively improve the LIBS emission. Firstly, this study discussed the spectra of FN DP LIBS with overlapping pulse time—that is, the FN DP inter-pulse delay (DID) was 0 μ s. The results showed that the spectra were increased to three times that of a single ns LIBS. Subsequently, the DID between the two pulses was optimized. The results showed that as the DID between the two pulses increased, the spectral emission first increased and then decreased, ultimately remaining unchanged. The optimized DID was approximately 2 μ s. Finally, using this optimized DID, the variation of spectral intensity with ns laser energy was discussed in DP LIBS. The spectral enhancement ratio increased from 3 with 0 μ s DID to 6 with 2 μ s DID. The investigation provides a reference in the application of FN DP LIBS element analysis.

Keywords: LIBS; fs + ns dual-pulse LIBS; single ns LIBS; spectral enhancement; plasma temperature

1. Introduction

Laser-induced breakdown spectroscopy (LIBS) is a technique that uses a high-power laser to vaporize a small amount of a sample and create plasma [1–3]. The light emitted by the plasma is detected by a spectrometer to obtain the element of the sample [4–6]. LIBS has many applications in fields such as material science, environmental monitoring, and forensic analysis. It is a non-destructive, fast, and highly sensitive analytical technique that can be used for qualitative and quantitative analysis.

Due to the fact that the sensitivity of traditional LIBS cannot meet the requirements of practical applications, how to improve LIBS analysis sensitivity has become a hot topic for many research groups [7–11]. One of the current studies on increasing the sensitivity is to improve the spectral emission of laser-induced plasma. Subsequently, various new LIBS detection technologies have emerged, and dual-pulse (DP) LIBS technology is one of them [12–15]. Its basic working principle is that the first laser pulse pre-excites the material to be tested, generating plasma. During the plasma expansion, the second pulse re-excites the plasma in the cooling state. Then, it detects the characteristic emission line of plasma induced by the second laser pulse. The DP LIBS technology generally has two types of laser path structures: collinear and orthogonal [16–18]. The collinear structure, also known as coaxial two pulses, refers to two parallel laser beams incident to sample surface and hitting the same position of the sample vertically in sequence. The orthogonal structure consists of two different working modes. The first laser is vertically incident on the target to be measured, generating plasma; the other laser pulse is parallel incident to the target surface to irradiate the plasma produced by the first laser vertically. Another method is for the first pulse to be incident parallel to the target surface to be tested, breaking down the air above the target surface, and then the other laser pulse to be incident perpendicular



Citation: Shao, J.; Zhang, Y.; Chen, A. Emission Enhancement in fs + ns Dual-Pulse LIBS of Cu. *Photonics* **2023**, *10*, 783. <https://doi.org/10.3390/photonics10070783>

Received: 5 June 2023

Revised: 27 June 2023

Accepted: 30 June 2023

Published: 5 July 2023



Copyright: © 2023 by the authors. Licensee MDPI, Basel, Switzerland. This article is an open access article distributed under the terms and conditions of the Creative Commons Attribution (CC BY) license (<https://creativecommons.org/licenses/by/4.0/>).

to the surface of the target. This method is similar to the single pulse LIBS of placing the sample in vacuum, because the first pulse breaks down the air above the target, reducing the air pressure on the target surface.

Femtosecond (fs) and nanosecond (ns) DP LIBS have promising application prospects in various fields. The ultrafast fs pulse can generate a plasma with a higher electron density, higher temperature, and lower ionization threshold, enabling the detection of trace elements and molecular species with high sensitivity and accuracy [19–21]. The ns pulse can generate a plasma with a longer emission duration, facilitating the detection of atomic species with a high ionization potential [22–24]. By combining the two pulses, fs and ns, DP LIBS can improve the accuracy, precision, and reproducibility of quantitative elemental analysis, reduce matrix effects and spectral interferences, and enhance the depth profiling capability of LIBS. Fs and ns DP LIBS has the potential to become a versatile analytical tool, such as in situ analysis of rocks and minerals, monitoring of toxic metals in environmental samples, and label-free analysis of tissue samples in biomedical research [25–27]. Zhao et al. used fs and ns DP to analyze the lead in soil [28], finding that the DP LIBS could increase the detection sensitivity of lead element in soil. Santagata et al. reported the detected response of fs and ns DP due to the orthogonal re-exciting induced by an ns laser on an fs laser excitation plume [29]. Lin et al. measured radical species of gas mixtures using fs and ns DP LIBS [30], and they believed that this technique provided an opportunity to determine the radical species in remote LIBS detection. Chu et al. extended the detection range of LIBS by combining high-intensity fs laser pulses with high-energy ns laser pulses [31], finding that the detection distance had been extended by three times. Lu et al. studied the use of an ultraviolet fs and ns DP to enhance the detection capability of LIBS in the case of high spatial resolution [32]. Until now, although many studies have discussed fs and ns DP LIBS, in fact, discussions on this field are relatively lacking compared to single ns LIBS. Specifically, the effect of ns laser energy (the second pulse) on spectral emission enhancement and the corresponding optimization of inter-pulse delay have been rarely discussed, and there is almost no research discussing the electron temperature and corresponding physical mechanisms in fs and ns DP LIBS. Therefore, we also carried out this study on the fs and ns DP LIBS.

This paper used an fs laser as time zero, and fs + ns DP inter-pulse delay (DID) ranged from 0 to 20 μ s. We first compared the spectra from single ns LIBS and fs + ns DP LIBS with 0 μ s DID. Next, we measured the spectra for different DIDs, calculated the electron temperatures, and obtained the optimized inter-pulse delay.

2. Experimental Details

The collinear fs and ns DP LIBS experimental system mainly included two laser systems, a spectral detection system, a pulse delay generator, and a three-dimensional translation stage, as shown in Figure 1a. The laser sources were an ultrafast Ti:sapphire laser system (Libra-HE, Coherent, Santa Clara, CA, USA) with 800 nm output wavelength and 50 fs pulse width and an Nd:YAG laser system (Surelite III, Continuum, Milpitas, CA, USA) with 1064 nm output wavelength and 10 ns pulse width. Two laser beams were focused onto the surface of the sample (Cu, purity 99.99%) through two mirrors and a focusing lens (focal length is 100 mm). To improve the accuracy of spectral detection, the samples were installed on a computer-controlled 3D translation stage (PTZ8, Thorlabs, Newton, NJ, USA). The plasma emission was collected by another focusing lens (diameter is 50 mm, focal length is 70 mm) and converged into a fiber. The optical fiber guided the signal to a spectrometer (SP500i, PIActon, Princeton Instruments, Trenton, NJ, USA) and an ICCD (PI-MAX-4, 1024i, Princeton Instruments, Trenton, NJ, USA). The digital signal delay generator was used to control the inter-pulse delay between the femtosecond and nanosecond laser pulses. The timing diagram of the experimental system was displayed in Figure 1b, and the fs laser signal was considered as time zero reference point. The experiment was conducted in the air, and each spectrum was generated from the accumulation of 100 laser irradiations.

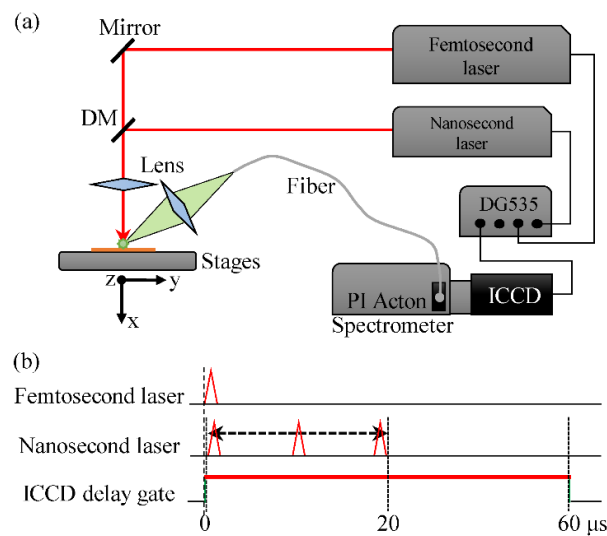


Figure 1. Experimental schematic (a) and timing diagrams (b).

3. Results and Discussion

Figure 2 compares the Cu (I) spectra at 510.55 nm, 515.32 nm, and 521.82 nm from single ns and fs + ns DP laser-produced copper plasmas. The fs + ns DID is 0 μs ; that is to say, these two laser beams coincide in time. For single ns LIBS, laser pulse energy has an influence on spectral emission. Increased laser pulse energy can cause the target material to absorb more energy, increasing laser-ablated plasma emission. This can also be observed from increased continuous spectra in Figure 2. In addition, the Cu spectra with fs + ns DP are stronger than those with single ns. The fs + ns DP with 0 μs inter-pulse delay displays a pronounced enhancement in the optical emission for all spectral lines. The obtained enhancement ratio is approximately 3, as shown in Figure 3. The enhancement mechanism of fs + ns DP LIBS is believed to be a combination of several factors, including (1) Plasma formation and confinement: the femtosecond pulse initiates the plasma formation, which is then confined by the nanosecond pulse. This confinement leads to a higher plasma density and a longer lifetime, which results in more atomic emissions. (2) Laser-induced breakdown threshold reduction: the femtosecond pulse can reduce the laser-induced breakdown threshold of the target, resulting in easier plasma formation and larger plasma volume. (3) Multi-photon excitation: the femtosecond pulse can lead to up to several orders of magnitude higher excitation for some species via multi-photon ionization. This higher excitation results in more atomic emissions. (4) Cascaded energy transfer: the femtosecond pulse can transfer energy to the surrounding gas, which then transfers the energy to the target through collisional processes. This cascaded energy transfer can enhance the atomic emission from the target.

Overall, the combination of these factors leads to a significant enhancement of the LIBS signal. The overlapping of the two laser pulses in time results in a more efficient ionization of the sample, leading to improved plasma emission. Furthermore, the shorter fs pulse can effectively reduce the influence of local thermal effects that can occur during ns laser pulse irradiation. This combination of fs and ns lasers in DP LIBS has the potential to improve the detection and analysis of materials in a wide range of fields. Also, the DID is important for DP LIBS to improve plasma emission. Subsequently, this study optimized the DID, hoping to enhance spectral emission through this optimization further.

Figure 4 shows the evolution of Cu (I) 521.8 nm peak intensity with increasing the DID in fs + ns dual-pulse LIBS. The variation characteristics of the signal of the spectral line can be divided into three different regions within the experimentally measured relative DID from 0 μs to 20 μs : the first region, as the DID ranges from 0 μs to 2 μs , shows that the line peak intensity varies with increasing the DID, and it continues to grow; at the DID of 2 μs , the intensity reaches a maximum value; when the DID changes from 2 μs to 10 μs , the

intensity starts to decrease; for the DID of 10–20 μs , that is the third region, the emission intensity remains unchanged in this region. The measurement of all Cu (I) spectral lines shows that the evolution trend of the emission peak intensity with the DID is consistent. The fs + ns DP LIBS is a technique that utilizes two laser pulses, one fs, and the other ns, to enhance the LIBS signal. The fs laser is used to create a plasma with a large number of atoms in highly excited states, while the ns laser re-excites the plasma to promote atomic emission. Combining two pulses results in a significant emission enhancement of the LIBS. An ns pulse after the fs pulse creates a more stable plasma that generates a stronger signal. And the fs pulse creates a micro-plasma on the target, increasing the ns pulse’s ablation efficiency.

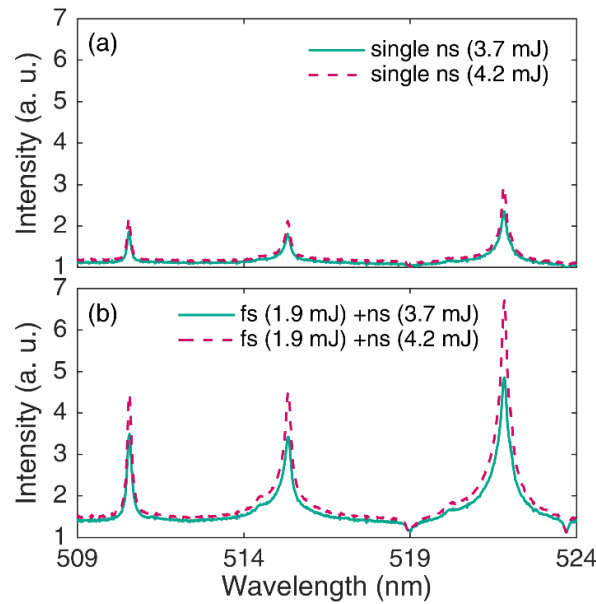


Figure 2. Single ns LIBS (a) and fs + ns LIBS with 0 μs inter-pulse delay (b).

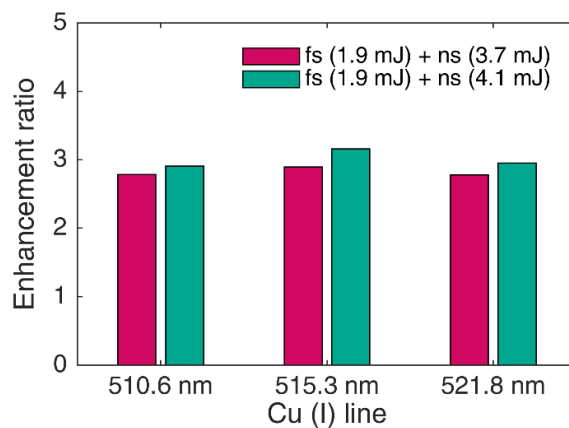


Figure 3. Comparison of enhancement ratio of Cu (I) line in fs + ns dual-pulse LIBS for different ns laser energies.

Electron temperature is an important parameter in understanding the process of laser-induced plasma [33]. The electron temperature can affect the plasma formation and evolution, as well as the spectral emission from plasma [34]. The electron temperature was calculated by the Boltzmann plot with the Cu (I) 510.55 nm, 515.32 nm, and 521.82 nm [35–38]. Figure 5 shows electron temperature evolution with the DID in fs + ns DP LIBS. The electron temperature has a similar trend with the 521.82 nm peak intensity (see Figure 4). When the DID is increased, the electron temperature rises, then drops, and remains relatively stable after 10 μs . For the DID of 0 μs , the DP is similar to a single pulse,

the DP re-excitation can be ignored, so the spectral signal and electron temperature are lower. As the DID is longer than 0 μs , the spectral signal and electron temperature rapidly reach the maximum. First, the fs laser generates a plasma plume, which rapidly expands on the surface of the sample at 0–2 μs . The subsequent ns pulse radiates the plasma, and when its pulse width is longer, the energy absorbed by the plasma is greater, and the plasma will contain more thermal particles. The ns pulse interacts with the expanding plasma, increasing the electron temperature of the excited species, thus producing stronger plasma emission intensity. At 2 μs , the plasma plume expands sufficiently to cover the spot size of the ns laser pulse. The absorption of laser energy reaches its maximum value, and the spectral emission becomes its maximum value. After 2 μs , the density of fs laser-induced plasma due to plume expansion begins to decrease. The absorption of nanosecond laser energy begins to weaken, leading to a decrease in plasma emission accordingly. When the delay reaches 10 μs , the plasma is so weak that it almost disappears. The subsequent ns laser begins to directly irradiate the target surface after the fs laser ablation, which is nearly equivalent to two separate pulses irradiating the surface of the sample separately. Therefore, the overall spectral emission remains unchanged.

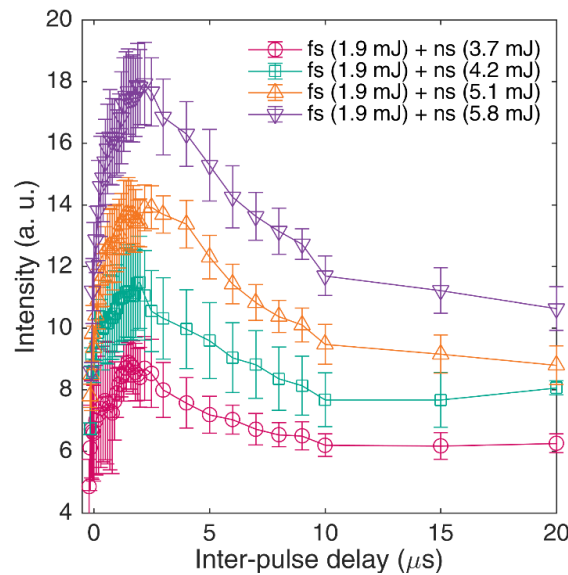


Figure 4. Evolution of Cu (I) 521.8 nm peak intensity with inter-pulse delay in fs + ns dual-pulse LIBS.

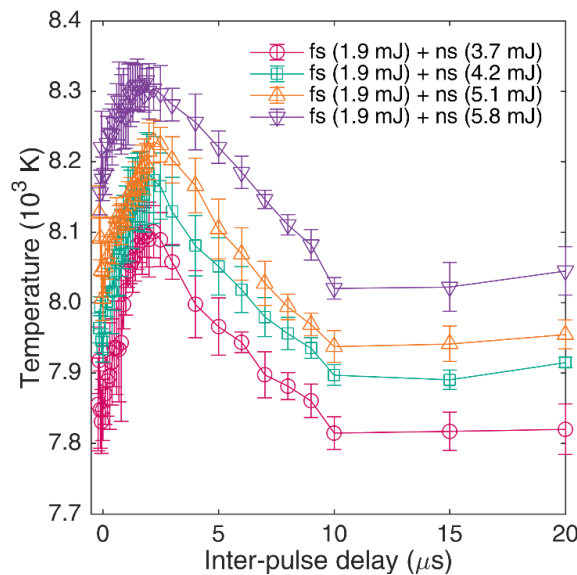


Figure 5. Evolution of electron temperature with inter-pulse delay in fs + ns dual-pulse LIBS.

Figure 6 shows the evolution of Cu (I) 521.8 nm peak intensity with increasing ns laser energy for single ns pulse LIBS, fs + ns DP LIBS with 0 μs DID, and fs + ns DP LIBS with optimized DID. It can be clearly observed that the emission signal produced by the optimized DID lasers is more pronounced with increasing ns pulse energy. The first fs laser ablates the target, generating a plasma. The subsequent ns pulse re-excites the plasma. When increasing the ns energy, the plasma will obtain more energy, increasing the excited particle number. Therefore, the spectral signal becomes stronger.

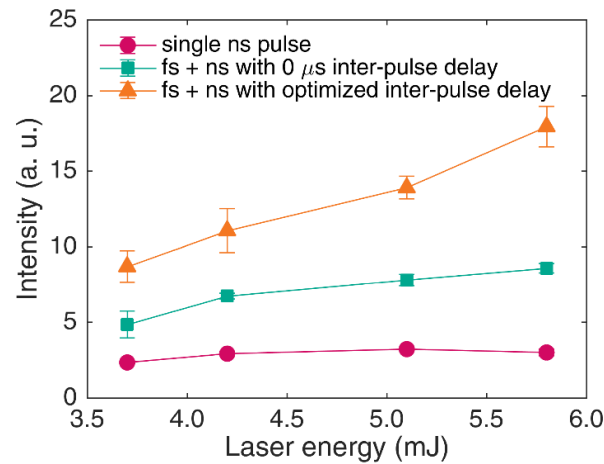


Figure 6. Evolution of Cu (I) 521.8 nm peak intensity with ns laser energy.

The relative standard deviation (RSD) is a commonly utilized metric in signal analysis to assess the precision and repeatability. In the context of LIBS, researchers place significant importance on the repeatability of measurements, as it is a crucial factor for achieving widespread commercialization of the technique. Reliable and reproducible results are vital to ensure consistent and accurate analysis in LIBS applications. Figure 7 shows the RSD of Cu (I) 521.8 nm peak intensity in fs + ns dual-pulse LIBS for different ns laser energies. For higher ns laser energies, the RSDs in fs + ns dual-pulse LIBS are lower compared to the case of single ns laser, and are less than 10%. This indicates that fs + ns dual-pulse LIBS has good signal repeatability.

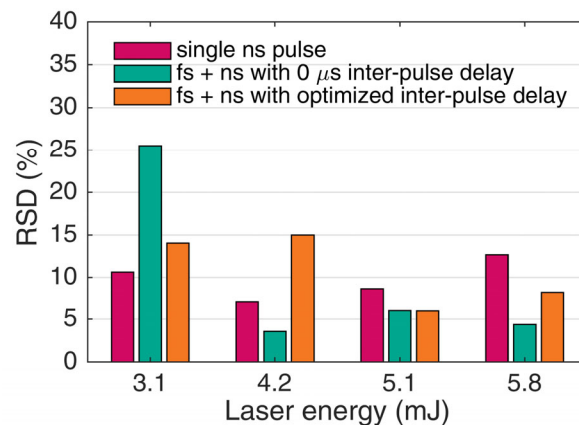


Figure 7. Comparison of RSD of Cu (I) 521.8 nm peak intensity in fs + ns dual-pulse LIBS for different ns laser energies.

In addition, the enhancement ratio was calculated from fs + ns DP LIBS divided by single ns LIBS, as presented in Figure 8. The optimized DP inter-pulse delay has increased the enhancement ratio from 3 to 6. In DP LIBS, the fs laser has many advantages as the first pulse over single ns LIBS: (1) Improved spatial resolution: fs laser pulses allow the formation of a small, intense plasma, resulting in improved spatial resolution and increased precision in the analysis of small features. (2) Reduced spectral interference: fs

pulses generate less spectral interference, which can reduce errors in quantitative analysis. (3) Widened elemental coverage: fs lasers can detect lighter elements, such as lithium and beryllium, which are challenging to measure with ns LIBS. (4) Reduced sample damage: with shorter pulse durations, fs lasers are less likely to cause damage or alteration to the sample surface, making them helpful in analyzing delicate samples. Using fs + ns DP LIBS, the disadvantage of fs LIBS will be overcome by re-exciting the plasma with ns pulses, and its disadvantage is a lower emission signal due to the ignored interaction between the excitation laser and the plasma. This is why the ns pulses are used to re-excite the plasma to achieve signal enhancement. Overall, using fs + ns DP LIBS can improve the accuracy, precision, and speed of elemental analysis in various applications.

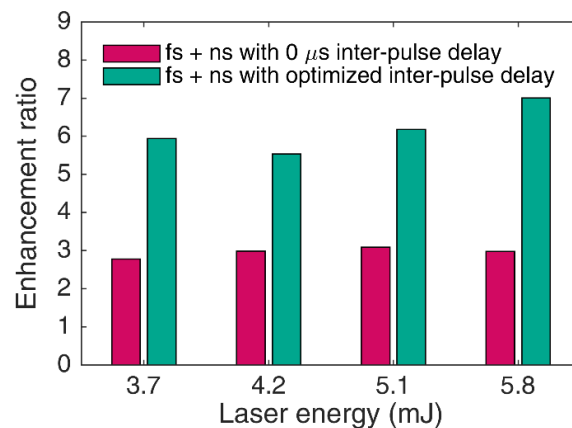


Figure 8. Comparison of enhancement ratio of Cu (I) 521.8 nm peak intensity in fs + ns dual-pulse LIBS for different ns laser energies.

4. Conclusions

This paper investigated collinear fs and ns DP LIBS due to the simple structure and suitability for long-distance detection in collinear DP LIBS. The fs laser was used as time zero, and the fs + ns DID range was from 0 to 20 μ s. Firstly, we compared the Cu (I) lines produced by single ns and fs + ns DP with 0 DID, indicating that the emission intensity of fs + ns DP LIBS had increased to three times that of single ns LIBS. Secondly, we measured the spectra for different DIDs, and calculated the electron temperatures. It was found that the spectral intensities and electron temperatures with the increase of the DID first increased and then decreased, and ultimately remained unchanged. At approximately 2 μ s DID, the spectral intensity and electron temperature were the highest. Finally, we discussed the evolution of spectral emission with the increase of ns laser energy by using the 2 μ s inter-pulse delay. The spectral enhancement ratio has been increased from 3 to 6 compared to single ns LIBS. The fs + ns DP LIBS has more advantages and can provide better application prospects in LIBS analysis.

Author Contributions: Conceptualization, J.S., Y.Z. and A.C.; methodology, J.S., Y.Z. and A.C.; software, J.S., Y.Z. and A.C.; validation, J.S., Y.Z. and A.C.; writing—original draft preparation, J.S., Y.Z. and A.C.; writing—review and editing, J.S., Y.Z. and A.C.; project administration, J.S. and A.C.; funding acquisition, A.C. All authors have read and agreed to the published version of the manuscript.

Funding: The research was supported by the National Natural Science Foundation of China (Nos. 11674128 and 11974138).

Institutional Review Board Statement: Not applicable.

Informed Consent Statement: Not applicable.

Data Availability Statement: The data presented in this study are available on request from the corresponding author. The data are not publicly available due to the confidentiality.

Conflicts of Interest: The authors declare no conflict of interest.

References

1. Carter, S.; Fisher, A.; Garcia, R.; Gibson, B.; Marshall, J.; Whiteside, I. Atomic spectrometry update: Review of advances in the analysis of metals, chemicals and functional materials. *J. Anal. Atom. Spectrom.* **2016**, *31*, 2114–2164. [[CrossRef](#)]
2. Winefordner, J.D.; Gornushkin, I.B.; Correll, T.; Gibb, E.; Smith, B.W.; Omenetto, N. Comparing several atomic spectrometric methods to the super stars: Special emphasis on laser induced breakdown spectrometry, libs, a future super star. *J. Anal. Atom. Spectrom.* **2004**, *19*, 1061–1083. [[CrossRef](#)]
3. Dong, P.-K.; Zhao, S.-Y.; Zheng, K.-X.; Wang, J.; Gao, X.; Hao, Z.-Q.; Lin, J.-Q. Rapid identification of ginseng origin by laser induced breakdown spectroscopy combined with neural network and support vector machine algorithm. *Acta. Phys. Sin. Ch. Ed.* **2021**, *70*, 040201.
4. Zhang, F.; Wang, Q.; Jiang, Y.; Chen, A.; Jin, M. Effect of gold nanoparticle concentration on spectral emission of alo molecular bands in nanoparticle-enhanced laser-induced al plasmas. *J. Anal. Atom. Spectrom.* **2023**, *38*, 422–428. [[CrossRef](#)]
5. Wang, Q.; Dang, W.; Jiang, Y.; Chen, A.; Jin, M. Improving the emission intensity of laser-induced breakdown spectroscopy by tip discharge of a tesla coil. *J. Anal. Atom. Spectrom.* **2022**, *37*, 994–999. [[CrossRef](#)]
6. Wang, Q.; Dang, W.; Jiang, Y.; Chen, A.; Jin, M. Emission enhancement of femtosecond laser-induced breakdown spectroscopy using vortex beam. *J. Phys. B At. Mol. Opt. Phys.* **2022**, *55*, 095402. [[CrossRef](#)]
7. Lednev, V.N.; Sdvizhenskii, P.A.; Grishin, M.Y.; Nikitin, E.A.; Gudkov, S.V.; Pershin, S.M. Improving calibration strategy for libs heavy metals analysis in agriculture applications. *Photonics* **2021**, *8*, 563. [[CrossRef](#)]
8. Amador-Mejía, M.; Sobral, H.; Robledo-Martinez, A. Elemental analysis of heated soil samples using laser-induced breakdown spectroscopy assisted with high-voltage discharges. *Chemosensors* **2023**, *11*, 193. [[CrossRef](#)]
9. Wen, X.; Hu, Z.; Nie, J.; Gao, Z.; Zhang, D.; Guo, L.; Ma, S.; Dong, D. Detection of lead in water at ppt levels using resin-enrichment combined with libs-lif. *J. Anal. Atom. Spectrom.* **2023**, *38*, 1108–1115. [[CrossRef](#)]
10. Ikeda, Y.; Soriano, J.K.; Wakaida, I. Plasma emission intensity expansion of zr metal and zr oxide via microwave enhancement laser-induced breakdown spectroscopy. *J. Anal. Atom. Spectrom.* **2023**, *38*, 1275–1284. [[CrossRef](#)]
11. Zheng, L.-N.; Xuan, P.; Huang, J.; Li, J.-L. Development and application of spark-induced breakdown spectroscopy. *Spectrosc. Spect. Anal.* **2023**, *43*, 665–673.
12. Luo, H.; Shen, S.; Wang, Z.; Yan, J.; Deguchi, Y. Copper signal characteristics using collinear ls-dp-libs for underwater measurement. *J. Laser Appl.* **2023**, *35*, 022017. [[CrossRef](#)]
13. Li, C.; Wang, Q.; Chen, A.; Gao, X. Influence of inter-pulse delay on cn molecular emission from femtosecond-nanosecond double-pulse laser-induced breakdown spectroscopy of pmma. *Optik* **2022**, *270*, 170029. [[CrossRef](#)]
14. Li, Y.; Ge, P.; Chen, Y. Studies on target-induced enhancement in pre-ablation orthogonal double-pulse laser-induced breakdown spectroscopy. *Spectrochim. Acta Part B At. Spectrosc.* **2022**, *198*, 106572. [[CrossRef](#)]
15. Wang, Y.; Chen, A.; Zhang, D.; Wang, Q.; Li, S.; Jiang, Y.; Jin, M. Enhanced optical emission in laser-induced breakdown spectroscopy by combining femtosecond and nanosecond laser pulses. *Phys. Plasmas.* **2020**, *27*, 023507. [[CrossRef](#)]
16. Rashid, B.; Ahmed, R.; Ali, R.; Baig, M.A. A comparative study of single and double pulse of laser induced breakdown spectroscopy of silver. *Phys. Plasmas* **2011**, *18*, 073301. [[CrossRef](#)]
17. Skrodzki, P.J.; Becker, J.R.; Diwakar, P.K.; Harilal, S.S.; Hassanein, A. A comparative study of single-pulse and double-pulse laser-induced breakdown spectroscopy with uranium-containing samples. *Appl. Spectrosc.* **2016**, *70*, 467–473. [[CrossRef](#)]
18. Wang, Y.; Chen, A.; Li, S.; Sui, L.; Liu, D.; Tian, D.; Jiang, Y.; Jin, M. Enhancement of laser-induced fe plasma spectroscopy with dual-wavelength femtosecond double-pulse. *J. Anal. Atom. Spectrom.* **2016**, *31*, 497–505. [[CrossRef](#)]
19. Labutin, T.A.; Lednev, V.N.; Ilyin, A.A.; Popov, A.M. Femtosecond laser-induced breakdown spectroscopy. *J. Anal. Atom. Spectrom.* **2016**, *31*, 90–118. [[CrossRef](#)]
20. Wang, Q.; Chen, A.; Zeng, X.; Chen, Y.; Li, S.; Jiang, Y.; Gao, X.; Jin, M. Influence of spark discharge on Al(i) and alo spectra in femtosecond laser-induced aluminum plasmas. *J. Anal. Atom. Spectrom.* **2021**, *36*, 1112–1117. [[CrossRef](#)]
21. Liu, Y.; Wang, Q.; Jiang, L.; Chen, A.; Han, J.; Jin, M. Femtosecond laser-induced cu plasma spectra at different laser polarizations and sample temperatures. *Chin. Phys. B* **2022**, *31*, 105201. [[CrossRef](#)]
22. Zakuskin, A.S.; Popov, A.M.; Labutin, T.A. Shift of ionization equilibrium in spatially confined laser induced plasma. *J. Anal. Atom. Spectrom.* **2019**, *34*, 1975–1981. [[CrossRef](#)]
23. Jiang, Y.F.; Wang, T.; Yu, W.; Jin, M.; Guo, J.; Liu, X.S. Exploration of carrier-envelope phase dependence on the double ionization process of ar and n-2 in few-cycle laser fields. *Laser Phys.* **2014**, *24*, 065301. [[CrossRef](#)]
24. Hu, W.Q.; Shin, Y.C.; King, G. Early-stage plasma dynamics with air ionization during ultrashort laser ablation of metal. *Phys. Plasmas* **2011**, *18*, 093302. [[CrossRef](#)]
25. Kalam, S.A.; Murthy, N.L.; Mathi, P.; Kommu, N.; Singh, A.K.; Rao, S.V. Correlation of molecular, atomic emissions with detonation parameters in femtosecond and nanosecond libs plasma of high energy materials. *J. Anal. Atom. Spectrom.* **2017**, *32*, 1535–1546. [[CrossRef](#)]
26. Serrano, J.; Moros, J.; Javier Laserna, J. Molecular signatures in femtosecond laser-induced organic plasmas: Comparison with nanosecond laser ablation. *Phys. Chem.* **2016**, *18*, 2398–2408. [[CrossRef](#)]

27. Sunku, S.; Gundawar, M.K.; Myakalwar, A.K.; Kiran, P.P.; Tewari, S.P.; Rao, S.V. Femtosecond and nanosecond laser induced breakdown spectroscopic studies of nto, hmx, and rdx. *Spectrochim. Acta Part B At. Spectrosc.* **2013**, *79–80*, 31–38. [[CrossRef](#)]
28. Zhao, S.; Song, C.; Gao, X.; Lin, J. Quantitative analysis of pb in soil by femtosecond-nanosecond double-pulse laser-induced breakdown spectroscopy. *Results Phys.* **2019**, *15*, 102736. [[CrossRef](#)]
29. Santagata, A.; Spera, D.; Albano, G.; Teghil, R.; Parisi, G.P.; De Bonis, A.; Villani, P. Orthogonal fs/ns double-pulse libs for copper-based-alloy analysis. *Appl. Phys. A* **2008**, *93*, 929–934. [[CrossRef](#)]
30. Lin, C.-H.; Liang, Z.; Zhou, J.; Tsai, H.-L. Femtosecond and nanosecond dual-laser optical emission spectroscopy of gas mixtures. *Appl. Spectrosc.* **2014**, *68*, 222–225. [[CrossRef](#)]
31. Chu, W.; Zeng, B.; Li, Z.; Yao, J.; Xie, H.; Li, G.; Wang, Z.; Cheng, Y. Range extension in laser-induced breakdown spectroscopy using femtosecond–nanosecond dual-beam laser system. *Appl. Phys. B* **2017**, *123*, 173. [[CrossRef](#)]
32. Lu, Y.; Zorba, V.; Mao, X.L.; Zheng, R.E.; Russo, R.E. Uv fs-ns double-pulse laser induced breakdown spectroscopy for high spatial resolution chemical analysis. *J. Anal. Atom. Spectrom.* **2013**, *28*, 743–748. [[CrossRef](#)]
33. Zhang, S.; Wang, X.; He, M.; Jiang, Y.; Zhang, B.; Hang, W.; Huang, B. Laser-induced plasma temperature. *Spectrochim. Acta Part B At. Spectrosc.* **2014**, *97*, 13–33. [[CrossRef](#)]
34. Ajith, A.; Swapna, M.N.; Cabrera, H.; Sankaraman, S.I. Comprehensive analysis of copper plasma: A laser-induced breakdown spectroscopic approach. *Photonics* **2023**, *10*, 199. [[CrossRef](#)]
35. Wang, Q.; Liu, Y.; Jiang, L.; Chen, A.; Han, J.; Jin, M. Metal micro/nanostructure enhanced laser-induced breakdown spectroscopy. *Anal. Chim. Acta* **2023**, *1241*, 340802. [[CrossRef](#)]
36. Wang, Y.; Chen, A.; Wang, Q.; Sui, L.; Ke, D.; Cao, S.; Li, S.; Jiang, Y.; Jin, M. Influence of distance between focusing lens and target surface on laser-induced cu plasma temperature. *Phys. Plasmas* **2018**, *25*, 033302. [[CrossRef](#)]
37. Freeman, J.R.; Harilal, S.S.; Diwakar, P.K.; Verhoff, B.; Hassanein, A. Comparison of optical emission from nanosecond and femtosecond laser produced plasma in atmosphere and vacuum conditions. *Spectrochim. Acta Part B At. Spectrosc.* **2013**, *87*, 43–50. [[CrossRef](#)]
38. Chen, L.; Deng, H.; Xiong, Z.; Guo, J.; Liu, Q.; Li, G.; Shang, L. Investigation of shielding effects on picosecond laser-induced copper plasma characteristics under different focusing distances. *Photonics* **2021**, *8*, 536. [[CrossRef](#)]

Disclaimer/Publisher’s Note: The statements, opinions and data contained in all publications are solely those of the individual author(s) and contributor(s) and not of MDPI and/or the editor(s). MDPI and/or the editor(s) disclaim responsibility for any injury to people or property resulting from any ideas, methods, instructions or products referred to in the content.